A Time-dependent Slab Symmetric Ablation Model with Allowance for Transverse Expansion and Magnetic Confinement Effects

L.L. Lengyel, P.N. Spathis

IPP 5/50

December 1992

MAX-PLANCK-INSTITUT FÜR PLASMAPHYSIK

8046 GARCHING BEI MÜNCHEN

MAX-PLANCK-INSTITUT FÜR PLASMAPHYSIK

GARCHING BEI MÜNCHEN

A Time-dependent Slab Symmetric Ablation Model with Allowance for Transverse Expansion and Magnetic Confinement Effects

L.L. Lengyel, P.N. Spathis

IPP 5/50 December 1992

Die nachstehende Arbeit wurde im Rahmen des Vertrages zwischen dem Max-Planck-Institut für Plasmaphysik und der Europäischen Atomgemeinschaft über die Zusammenarbeit auf dem Gebiete der Plasmaphysik durchgeführt.

A time-dependent slab symmetric ablation model with allowance for transverse expansion and magnetic confinement effects

L.L. Lengyel and P. Spathis

Max-Planck-Institut für Plasmaphysik
D-8046 Garching bei München, Germany.

Abstract

A self-consistent, time-dependent, slab-symmetric ablation model has been developed. Two time-dependent 1.5-D variable mass Lagrangian codes are coupled which are based on the full set of conservation equations with mass-source terms present, and on Maxwell's equations. Each code has its principal direction: the direction of the magnetic field and the one perpendicular to it. The energy deposition in the shielding cloud is determined by stopping length calculations applied along the magnetic field lines with allowance for electrostatic shielding effects. The stopping length calculations are supplemented by thermal diffusion calculations, thus redistributing the energy deposited in the discrete energy group approximation. The neutral cloud is allowed to expand also in the direction perpendicular to the magnetic field. The deceleration and full stopping of this motion are calculated by means of an MHD model (iteratively with the axial expansion dynamics), thus determining the transient variation of the lateral cloud dimension. The time variation of the ablation rate as well as its value averaged over the residence time of a pellet (of given injection velocity) in a flux tube defined by the ionization radius of the ablatant are presented and compared with results stemming from known steady-state ablation models.

Introduction

A pellet injected into a thermonuclear plasma will suddenly be exposed to the direct action of energetic particles. For a short period of time, the pellet behaves like a solid obstacle immersed in a plasma. If the energy of the incident particles is sufficienly high (as in the case of suprathermal electrons), their penetration is deep and volumetric energy deposition occurs. In the case of thermal plasmas and owing to the difference in the thermal velocities of electrons and ions, the pellet surface will first gain a negative excess charge, which reduces the incident electron flux and increases the ion flux at the pellet surface until the two become equal. This pre-heating period, with duration in the sub-μs range, ends when the particle energy in the surface layers reaches values corresponding to the sublimation energy of the pellet substances considered (ϵ_{sbl} = 7.5 eV and 1.6 eV for C and Li, respectively, compared with $\epsilon_{sbl} = 0.005$ eV per atom in the case of hydrogen). At this time, the second phase, characterized by intense removal of atomic or molecular layers from the pellet surface, viz. ablation, begins. The pellet erodes or "ablates" at a rate that is defined by the balance between the energy flux reaching the pellet surface and the flux that is required to remove particles from the surface and dissociate, ionize, and carry them away from the surface.
At some time instant, the cloud particles begin to become ionized and to interact with the magnetic field, i.e. their radial expansion becomes decelerated and eventually comes to a full stop. The stopping times are measured on the Alfvén time scale and are in the microsecond range [1, 2]. For tokamak plasma parameter ranges of present interest, the stopping radii vary in the millimetre (up to cm) range. The expanding, partially or fully ionized ablatant cloud may distort the magnetic field: a transient magnetic cavity may form inside the cloud. This radial deceleration and gradual confinement phase is followed by a quasi-steady phase associated with the field-aligned expansion of the ablatant, which involves much longer hydrodynamic time scales. In general, the duration of this phase is determined by the residence time of the pellet in its own radially confined ablatant cloud [2, 3]. For the pellet velocities now used it is of the order of 10 μs. Hence the ablation process is an inherently transient process.

Experiments [3, 4] and model calculations [2] indicate that the shielding cloud surrounding the pellet is cigar-shaped and of high density and low temperature. Considerable gradients exist within the cloud both in the B-parallel and B-perp directions. During pellet injection, a pronounced periodic modulation of the H_α radiation emitted by the ablated, but not yet ionized pellet particles is usually observed [3, 4]. The wavelength of these modulations (measured along the pellet path) was found to be

approximatelly given by the ionization length of the ablated particles. This oscillatory pattern is thus most likely due to the periodic crossing of the pellet through the boundaries (ionization radius) of its own shielding cloud. Since the pellet ablates continuously and the neutral gas produced precedes the pellet all the time, the formation of the new cloud upon exit of the old one is not an abrupt process. The resulting oscillations both in the shielding cloud properties and in the ablation rate are damped to a certain extent.

There exist presumptions according to which the ionized portion of the cloud, or a substantial fraction of it, moves with the pellet because of a polarization-induced drift motion (see, for example, [5]), thus enhancing the inward-directed pellet particle transport. However, there is neither convincing theory nor experimental evidence to prove this proposition. On the contrary, experimental observations indicate that, if enhanced particle deposition due to cloud drift occurs at all, then at the plasma periphery [6, 7], most likely due to outward-directed high-beta drift of the cloud in the toroidal magnetic field [8]. Furthermore, in analogous cases encountered in extraterrestrial plasmas the polarization field has been shown to be shorted out [9].

The magnitude of the energy flux affecting the pellet and its environment depends on several concurrent processes: collisional energy transfer from the incident plasma particles to the ablated and expanding pellet substance, development of a self-regulating ambipolar electrostatic field in the shielding cloud assuring zero net current and thus preventing unbalanced charge accumulation, and possible distortion of the confining magnetic field by the ablated ionized and expanding pellet substance. The magnetic field affects the ablation process in two ways: first, the incident energy carriers are confined to magnetic flux lines and thus any distortion of the magnetic field topology, e.g. possible formation of a diamagnetic bubble around the pellet, affects the energy flux available, and, secondly, magnetic confinement, i.e. funnelling of the ionized portion of the ablated substance, modifies the density distributions around the pellet and the associated collisional energy transfer rates (the line integral values that determine the gasdynamic shielding efficiencies). The heat flux affecting the shielding cloud in the transverse direction is usually negligible. However, in the case of surface instability, magnetic turbulence, and turbulent mixing at the cloud-plasma interface [10, 11], the magnitude of this flux component should be correctly assessed.

The ablation models now available are based on steady-state approximations [12, 13, 14, 15] and, with the exception of [15], on the assumption of spherically symmetric (zero magnetic field) hydrodynamic expansion. The latter model takes the confine-

ment of the ionized pellet substance into account by means of an assumed confinement radius, empirically retaining, at the same time, the major characteristics of the older spherically symmetric model. (A detailed analysis of these and other ablation models is given elsewhere [16].) As a result of the assumed spherical free expansion, transonic flow results with the supersonic domain extending to infinity. The energy flux incident on the pellet surface is modelled by monoenergetic electron beams in [12] and [13]. Kuteev [14] used an integral expression (based on the Bethe-Bloch approximation) for describing the energy loss of the incident electrons of different energies. In all these models, the effect of the magnetic field on the cloud evolution was postulated to be negligible from the very beginning [17]. A later analysis pertaining to the distortion of the magnetic field near the pellet by neglecting again the magnetic field effects in the first-order hydrodynamic parameter distributions [18] led to the same conclusion. Possible build-up of an ambipolar electrostatic field yielding additional shielding was also ignored, on the basis of initial estimates [19, 13], in these models. There are indications [20, 21] that electrostatic shielding effects may be notable. Although experimentally measured pellet penetration depths and other ablation characteristics were successfully reproduced by each of these ablation models, they may yield different results if applied to the same plasma scenario (see Figures 1a to 1c discussed in the following sections). Inspired by Rose's diamagnetic balloon model [22], Chang [23] and Lengyel [24] showed that the magnetic constriction of the ionized ablatant may indeed have a significant effect on the ablation process. While Chang's magnetic nozzle model had some inherent problems (for a discussion see [24]), further analyses aimed at the evolution of vapour clouds around ablating pellets [1, 2, 25] validated these presumptions and showed ageement with experimental observations.

In the following, a time-dependent ablation model is presented. The model is applied to a typical pellet injection scenario. The spatial variation of the ablation rate calculated and the penetration depth obtained are compared with those stemming from the available neutral gas shielding models.

A self-consistent ablation model

In view of the above arguments, in any realistic approximation aimed at modelling ablation, with some chance of qualifying for predictive calculations, the following facts should be taken into account (most of these arguments also hold for surface erosion problems caused by accidental plasma - wall contact):

(1) The rate of erosion/ablation of a surface is determined by the balance between the energy flux reaching the surface and the energy flux carried away from it by the eroded/ablated particles (sublimation energy plus initial enthalpy). The ablated particles form a shielding cloud at the eroding surface.

(2) The cloud is heated primarily by plasma particles confined to magnetic flux surfaces. The energy transport is not spherically symmetric. The energy carriers are not monoenergetic.

(3) The particles in the high-energy wing of the distribution function have the deepest penetration depth and thus play the major role in defining the parallel energy flux $q_{\parallel}$ and the flux balance at the eroding surface.

(4) Although the transverse energy flux affecting the cloud $q_{\perp}$ is, in general, negligible compared with $q_{\parallel}$, it affects processes taking place at the cloud-plasma interface, such as enhanced surface ionization and local interaction with the magnetic field. Since the length of the ablatant hose rapidly increases in time, $q_{\perp}$ may also affect phenomena measured on the time scale of the field-aligned expansion.

(5) Charged energy carriers of different initial energies penetrate to different depths in the cloud. The net charge distribution, including the effect of the ionized ablatant particles, sets up an ambipolar electric field such that the net electric current vanishes in any B-perp cloud cross-section. This electric field affects the incident flux of charged particles. An additional field (potential drop) may be generated at the cold cloud hot plasma interface [20].

(6) The ablated particles leave the pellet surface as neutrals. Their ionization time is defined by finite-rate atomic processes. No instantaneous ionization equilibrium exists in the shielding cloud. The beginning of the interaction of the ablatant with the magnetic field is determined by the ionization time.

(7) As a result of interaction with the magnetic field, the transverse expansion of the ablatant stops, resulting in a well-defined transverse ablatant hose dimension. This transverse dimension has a decisive effect on the build-up of the shielding properties (density, temperature) of the cold blanket forming around the pellet.

(8) The shielding cloud may represent a high-beta inclusion (blob) for the background plasma, depending on the energy supply rate available, the local ablation rate, and the magnetic field strength. The residence time of the pellet in this blob is given by the ratio of the cloud (confining flux tube) diameter and the pellet velocity (normal injection

is considered). The ablation rate varies during the residence time, the variation being due to the temporal variation of the shielding properties (mass accumulation in the flux tube, etc.) caused by the ablation itself.

(9) The ablation rate undergoes a cyclic change associated with the periodic exiting of the flux tubes confining the ionized ablatant. The characteristics of the new ablation cycle are determined by the energy fluxes and the magnetic field strength "seen" by the pellet after crossing the ionized shell of the old ablation hose.

The ablation model presented here comprises two parts each aimed at solving part of the whole problem:
(a) determination of the energy flux transported by plasma particles to the pellet surface along the magnetic field lines,
(b) determination of the shielding characteristics of the particle cloud evolving around the pellet.

For this purpose two time-dependent 1.5-D variable-mass Lagrangian codes were coupled, thus in fact replacing a rather complex 2-D code that would otherwise be necessary for solving the problem.
Both codes are based on the full set of coservation equations with mass-source terms present and are of the single-temperature single-velocity type. Each code has its principal direction: the direction of the magnetic field ("PARALEX") and the one perpendicular to it ("PERPEX"). The essential effects of the complementary direction are taken reciprocally from the other code, by means of iterative feedback coupling. In both codes, the calculations are performed with finite rate atomic processes: collisional and radiative ionization and recombination processes are taken into account. The rate coefficients used are given in [2, 26, 27].

The first code, PARALEX, being the actual ablation code, takes care of the processes associated with the direction of the magnetic field lines:
(a) Penetration of plasma particles into the shielding cloud, collisional energy transfer to the cloud particles, particle and energy flux depletion calculations.
(b) Field-aligned electrostatic field calculations based on the zero net current condition in the direction parallel to B (not counting, of course, the discharge currents in the background plasma).
(c) Gasdynamic expansion of the ablatant along the magnetic field lines in a quasi-one-dimensional channel flow approximation. The effect of the complementary dimension manifested in the evolution of the transverse channel dimension is taken from the

second code.
(d) Variation of the ionization state of the species in time and space (along the magnetic field lines).

In this series of calculations, the Maxwellian energy distribution of the incident plasma particles was represented by 5 discrete energy groups. A detailed description of the first code, without the effects of the complementary dimension (transient expansion of the Lagrangian cells in the transverse direction, transverse heat conduction), is given in [26, 27]. This is the version used in the present calculations.

The second code, PERPEX, is a self-consistent MHD code based on the usual set of continuity equations and Maxwell's equations. The code calculates, for given background plasma parameters, magnetic field strength, and ablation rate,
(a) the expansion and ionization processes in the transverse direction;
(b) the magnitude of the induced $\vec{v} \times \vec{B}$-emf, the resulting azimuthal current density $\vec{j}$, and the associated deceleration force $\vec{j} \times \vec{B}$;
(c) the time variation of the cloud radius, the stopping time of the transverse expansion, and the confinement radius;
(d) the degree of diamagnetism (reduction of the magnetic flux in the cloud).
Since each Lagrangian cell used in these calculations is allowed to expand also in the axial direction (the expansion rates are calculated from the pressure values known on both sides of the cloud-plasma interface), the effect of the complementary dimension is thus also taken into account. Energy is supplied to the cloud by means of flux-limited thermal conduction along the magnetic field lines and by anomalous conduction in the transverse direction from the side of the ambient plasma. The transverse energy flux is in general negligible compared with the field-aligned value, but is sufficient for initiating the ionization at the cloud-plasma interface. The details of this code are given elsewhere [2, 25]. Noteworthy is that the ablation rate used in this second code is an input quantity obtained from the first (ablation) code.

With regard to the computational procedure:

The initial pellet and plasma parameters v_{pel}, r_{pel}, $n_e(r)$, $T_e(r)$ and the magnetic field strength B_0 are assumed to be given. The ablation rate is computed at a discrete number of positions in the plasma (flux surfaces in the case of tokamaks). At each position, the computations are performed in the following manner:

1. Assuming an ablatant cloud radius of the order of 1 cm, the first code, PARALEX, computes the time history of the ablation rate for a time interval of the order of

the residence time of the pellet within its own shielding cloud. The time variation of the ablation rate resulting from these calculations is approximated by an analytic function and transferred to the second code, which calculates the transverse expansion dynamics.

2. For the ablation rate thus described and an energy input rate specified in terms of the background plasma parameters, the details of the transverse expansion are calculated by PERPEX. The resulting major output parameters τ_{stp}, R_{cld}, $v_\perp$, and B/B_0 (magnetic shielding factor) are transferred back to the first code.

3. The ablation rate is now recalculated (PARALEX) by using the calculated channel radius R_{cld} and stopping time τ_{stp}. If magnetic shielding takes place, the input energy flux is accordingly corrected by the B/B_0 factor. Finally, the updated value of the ablation rate function is determined.

4. Steps (2) and (3) are repeated in an iterative manner until the final value of the ablation rate (a time function) is obtained. The convergence of this procedure was found to be rather good: in these preliminary calculations 2 or 3 iterations always sufficed.

5. Knowing the ablation rate, one can estimate the change of the pellet size over the pellet flight path to the next station (tokamak flux surface) considered. Procedure (1) to (4) is repeated at the next flux tube and the pellet is further advanced The calculation is terminated when the pellet mass vanishes (its radius reduces to zero).

Results of calculations

As a representative scenario, a plasma the size of an ASDEX-UP discharge with a = 50 cm, $T_{e0} = 1.5$ keV, $n_{e0} = 3 \times 10^{19}\ m^{-3}$, and B = 3 tesla was selected. The spatial variations of T_e and n_e were prescribed by means of the usual power-law dependence: $(1-(r/a)^a)^b$, with a = b = 2 for T_e and a = 2, b = 1 for n_e. The size of the pellet injected was $r_{pel} = 1$ mm, the injection velocity $v_{pel} = 1200$ m/s.

For the purpose of comparison, we first computed the expected spatial variation of the ablation rate and the corresponding penetration depth by means of three neutral gas shielding ablation models available. Figures 1a to 1c represent the results of these calculations and correspond to [12], [13], and [14], respectively. (The figures were provided by F.X. Söldner, who computed them with the help of the ablation code and software EVAPMODL, developed by B. Kuteev and co-workers at St. Petersburg Techn. University.) The difference between the ablation rates and penetration depths

computed by the three different models is notable.

With regard to the present calculations, the ablation rate and the associated pellet size reduction were determined sequentially at a descrete number of radial positions along the pellet path. At each position, first a cloud radius was assumed ($R_{cld} \approx 1\ cm$) and the time-dependent ablation rate corresponding to this cloud radius and the local plasma parameters $T_e(r)$, $n_e(r)$ was calculated with the help of PARALEX. The time variation of the resulting ablation rate was described empirically for the first 10 μs of the ablation time by two exponential functions of the type $\dot{N} = a_0 \cdot exp(-t/b_0)$ for $0 \leq t \leq 5\ \mu s$, and $a_1 \cdot exp(-t/b_1)$ for $5 \leq t \leq 10\ \mu s$ (t represents the physical time in μs, and a_0, a_1, b_0, and b_1 are empirical constants). Next, the ablation rate functions thus obtained were transferred to the PERPEX transverse expansion program. The time history of the transverse expansion was now calculated. The major results of these calculations are the confinement radius (i.e. cloud radius) R_{cld}, the associated stopping time τ_{stp}, and the magnetic shielding factor B/B_0.

With the calculated values of the cloud radius R_{cld}, stopping time τ_{stp}, and magnetic shielding factor B/B_0 the ablation rate can now be recalculated by means of PARALEX. In general, the pellet cross-section $\pi {r_{pel}}^2$ is considerably smaller than the cloud cross-section $\pi {R_{cld}}^2$. The gradual expansion of the flux tube cross-section from $\pi {r_{pel}}^2$ to $\pi {R_{cld}}^2$ is characterized by the stopping time τ_{stp}. In the present series of calculations, it was assumed that the particles set free at the pellet surface instantaneously fill the whole channel cross-section, i.e. the stopping-time value was not used. Such an approximation corresponds to the lower limit of the attainable shielding effect: in reality, the transverse expansion rate of the ablated particles is finite and thus for a given ablation rate the pile-up of the particles in the neighbourhood of the pellet is more pronounced, resulting in stronger shielding. (In a further version of this model, the time variation of the effective channel cross-section caused by the transverse expansion of the ablatant will be taken into account.)
The resulting new ablation rates can again be represented by exponential functions and transferred to PERPEX for determining the corrected values of the cloud radius, etc.

Figure 2 shows the variation of the transverse dimension of the ablatant cloud (approximatelly equal to the ionization radius) along the pellet path. At the periphery of the plasma, the plasma temperature is low and the ionization time of the ablated particles is relatively long. A relatively large cloud radius (in agreement with the dif-

fuse cloud structure experimentally observed at the plasma periphery) results. As the pellet penetrates further inward, the ionization time becomes shorter and a continuously decreasing cloud radius results. Accordingly, the cloud density is rather low at the plasma periphery, yielding poor shielding, and notably higher at magnetic flux surfaces located closer to the plasma centre resulting in more efficient shielding there. The local ablation rate is defined by the combination of the energy flux available and the shielding efficiency of the cloud.

The variation of the ablation rate along the pellet path, computed in the five-energy-group approximation, is shown in Fig. 3. The values displayed correspond to local ablation rates averaged over the first 10 μs of the residence time of the pellet at each radial position. Due to the rather limited number of radial positions taken (8 altogether), the curve can only be considered as approximate. For the sake of comparison, the ablation curve corresponding to a single-energy-group approximation (Maxwellian energy distribution, on the average $2kT_{e0}$ energy per incident plasma electron) is shown as a dotted line in the same figure. The difference between the single-energy and multi-energy-group approximations is substantial: while the single-energy-group approximation predicts pellet penetration well beyond the torus axis, the multi-group approximation yields a penetration depth of about 35 cm. The neutral gas shielding ablation models predict similar penetration depths for this particular magnetic field strength (3 tesla). The ablation curve computed does not show any substantial shift towards the plasma periphery, in spite of the reduced shielding efficiency in the peripheral region. Apparently, in the case of the scenario considered, the variation of the energy flux affecting the pellet with the plasma radius overrides the change of the shielding efficiency along the pellet path.

References

[1] LENGYEL, L.L, Phys. Fluids **31** (1988) 1577.

[2] LENGYEL, L.L., ZAVALA, G.G., KARDAUN, O.J., and LALOUSIS, P., Nucl. Fusion **31** (1991) 1107.

[3] DURST, R.D., ROWAN, W.L., AUSTIN, M.E., et al., Nucl. Fusion **30** (1990) 3.

[4] WURDEN, G.A., BÜCHL, K., at al., Rev. Sci. Instr. **61** (1990), 3604.

[5] FISHER, R.K., McCHESNEY, J.M., HOWALD, A.M., PARKS, P.B., and THOMAS, D.M., Rev. Sci. Instr. **61** (1990) 3196.

[6] SCHMIDT, G.L., BARTLETT, D., and BAYLOR, L., Int. Conf. Pl. Phys. (Proc. 19th EPS Conf. Innsbruck 1992) **16C** Pt.I 255.

[7] BAYLOR, L.R., SCHMIDT, G.L., et al., Nucl. Fusion **32** (1992), 2177.

[8] LENGYEL, L.L., Nucl. Fusion **17** (1977), 805.

[9] BOROVSKY, J.E., IEEE Trans. Pl. Sci. **20** No.6 (Dec. 1992),in press.

[10] DIMONTE, G., and WILEY, L.G., Phys. Rev. Lett. **67** (1991), 1755.

[11] HUBA, J.D., BERNHARDT, P.A., and LYON, J.G., J. Geophys. Res. **97** (1992), 11.

[12] MILORA, S.L., and FOSTER,C.A., IEEE Trans. Pl.Sci. **PS-6** (1978) 578.

[13] PARKS, P.B., and TURNBULL, R.J., Phys. Fluids **21** (1978) 1735.

[14] KUTEEV, B.V., UMOV, A.P., and TSENDIN, L.D., Sov. J. Pl. Phys. **11** (1985) 236.

[15] HOULBERG, W.A., MILORA, S.L., and ATTENBERGER, S.E., Nucl. Fusion **28** (1988) 595.

[16] See section "Pellet Shielding and Ablation Physics" in "Review of Pellet Fuelling" by MILORA, S.L., HOULBERG, W.A., LENGYEL, L.L., and MERTENS, V., to appear in Nucl. Fusion (1993).

[17] PARKS, P.B., TURNBULL, R.J., and FOSTER, C.A., Nucl. Fusion **17** (1977), 539.

[18] PARKS, P.B., Nucl. Fusion **20** (1980), 311.

[19] FELBER, F.S., MILLER, P.H., PARKS, P.B., at al., Technical Report GA-A14960, General Atomic Co, San Diego, Cal. 1978.

[20] ISHIGURO, S.I., KAMIMURA, T., and SATO, T., Phys. Fluids **28** (1985), 2100.

[21] ROZHANSKY, V.A., Sov. J. Plasma Phys. **15** (1989), 638.

[22] ROSE, D.J., Culham Lab. Technology Div. Memo No. 82 (1968).

[23] CHANG, C.T., Nucl. Fusion **15** (1975), 595.

[24] LENGYEL, L.L., Phys. Fluids **21** (1978), 1945.

[25] LENGYEL, L.L., IEEE Trans. Pl. Sci. **20** No.6 (Dec. 1992), in press.

[26] SPATHIS, P.N., "Field aligned expansion of particle clouds in magnetically confined plasmas", Techn. Rept. IPP 5/38, Max-Planck-Institut für Plasmaphysik, Garching, 1992.

[27] SPATHIS, P.N., and LENGYEL, L.L., Int. Conf. on Pl. Phys. (Proc. 18th EPS Conf. Innsbruck 1992) **16C** Pt.I, 323.

[28] LENGYEL, L.L., Nucl. Fusion **29** (1989) 37.

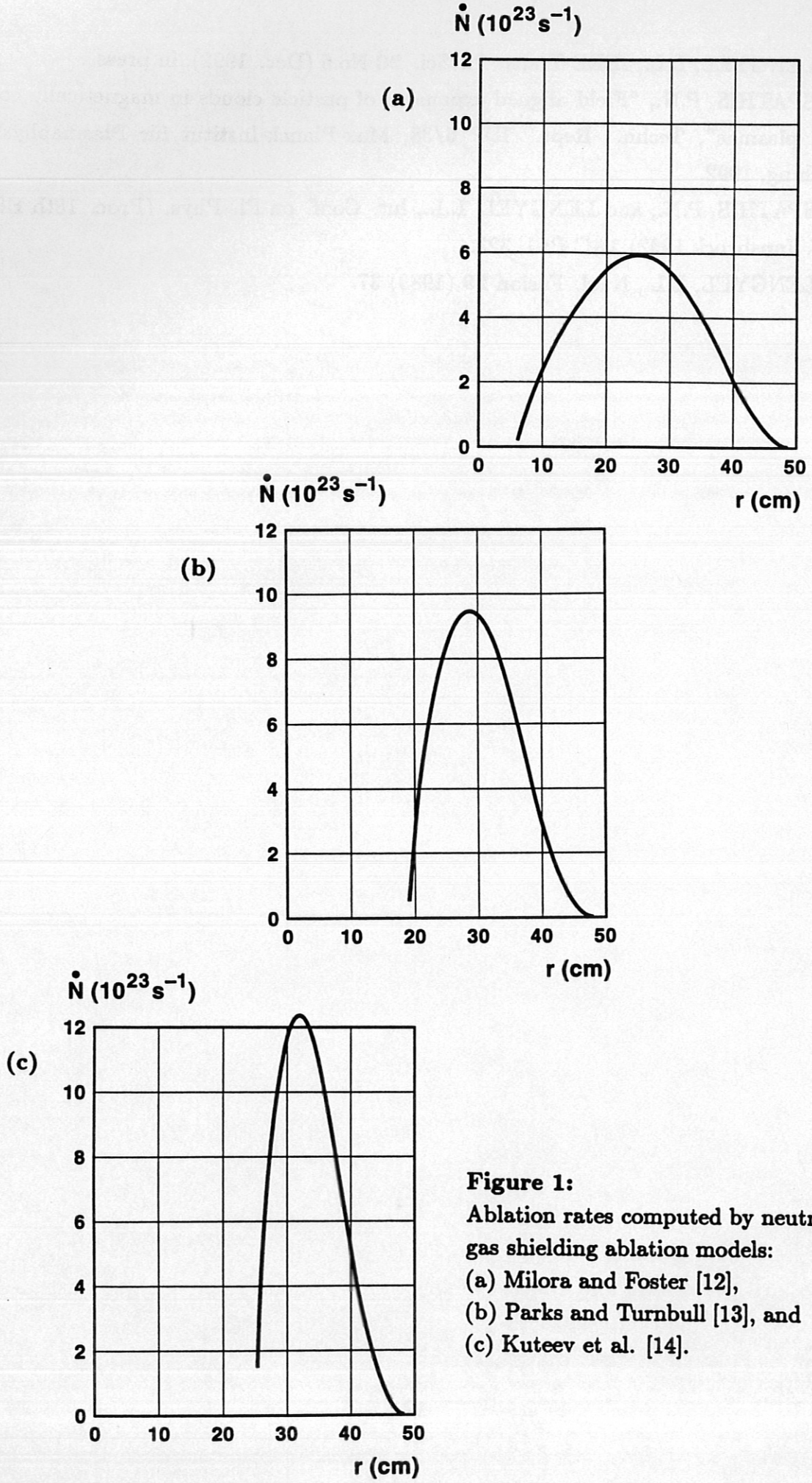

Figure 1:
Ablation rates computed by neutral gas shielding ablation models:
(a) Milora and Foster [12],
(b) Parks and Turnbull [13], and
(c) Kuteev et al. [14].

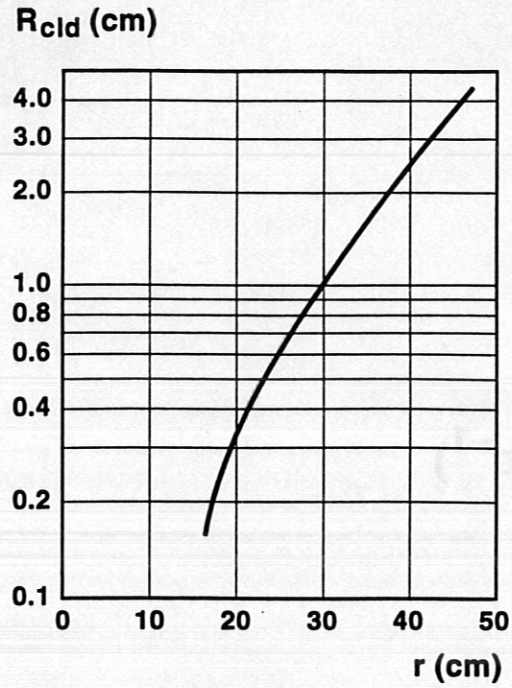

Figure 2: Variation of the shielding cloud radius R_{cld} along the pellet path computed in the present approximation.

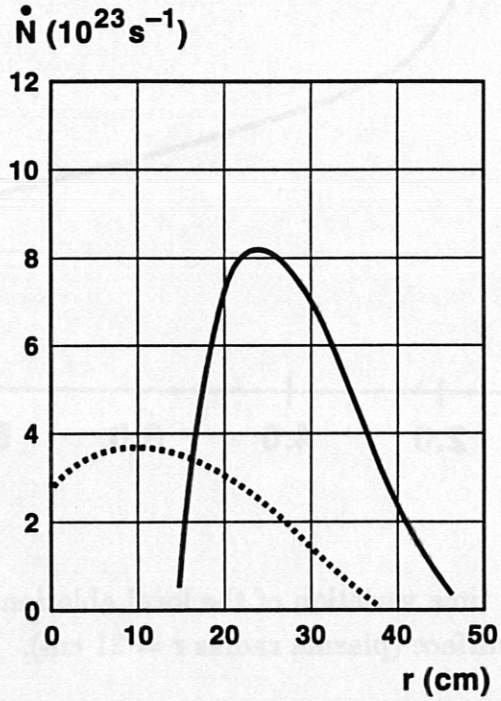

Figure 3: Variation of the local ablation rate (averaged over the first 10 μs of the residence time in the ablation cloud) along the pellet path (dotted line: single-energy-group approximation).

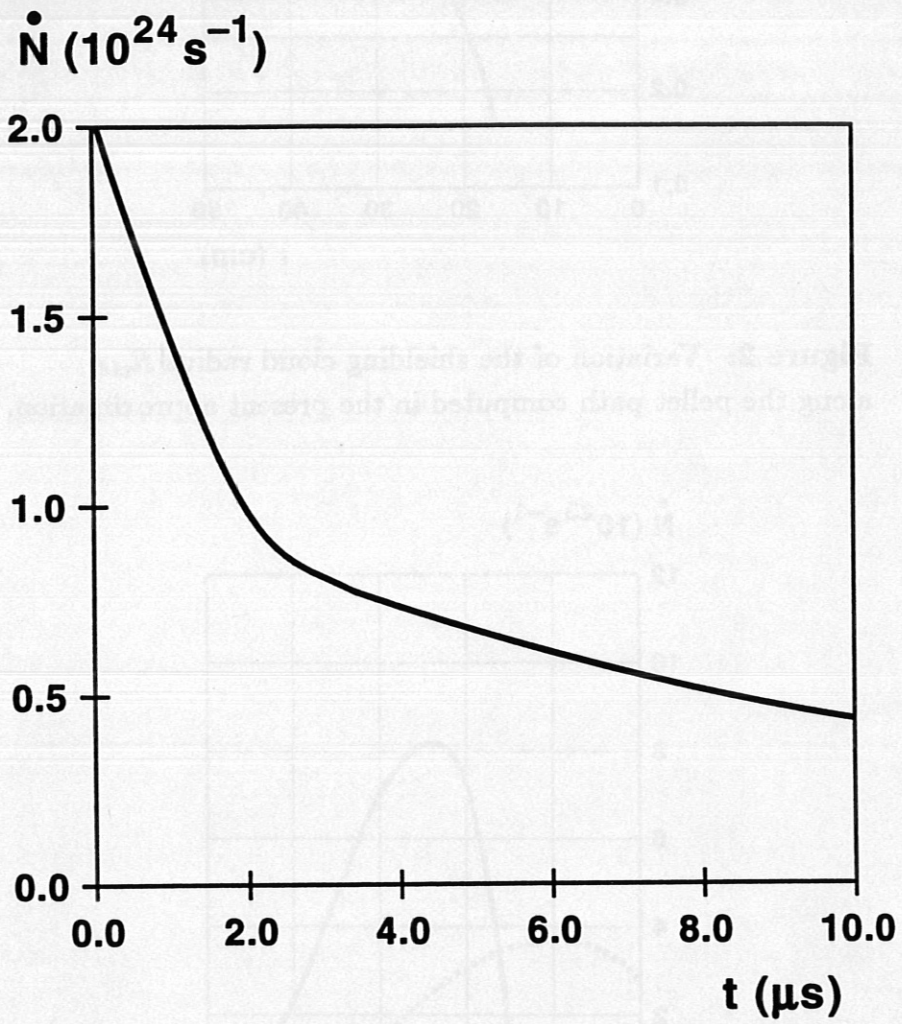

Figure 4: Typical time variation of the local ablation rate at a magnetic flux surface (plasma radius r = 21 cm).